Basic

Immunodeficiencies and autoimmunity

Research Article

Protection from EAE in DOCK8 mutant mice occurs despite increased Th17 cell frequencies in the periphery

Alicia S. Wilson[1], Hsei Di Law[1], Christiane B. Knobbe-Thomsen[2], Conor J. Kearney[3], Jane Oliaro[3], Carole Binsfeld[4], Gaetan Burgio[1], Lora Starrs[1], Dirk Brenner[4,5], Katrina L. Randall*[1,6] and Anne Brüstle*[1]

[1] The John Curtin School of Medical Research, The Australian National University, Canberra, Australian Capital Territory, Australia
[2] Department of Neuropathology, Heinrich Heine University Düsseldorf, Düsseldorf, Germany
[3] Immune Defence Laboratory, Cancer Immunology Division, The Peter MacCallum Cancer Centre, Melbourne, Australia
[4] Department of Infection and Immunity, Experimental and Molecular Immunology, Luxembourg Institute of Health, Esch-sur-Alzette, Luxembourg
[5] Odense Research Center for Anaphylaxis, Department of Dermatology and Allergy Center, Odense University Hospital, University of Southern Denmark, Odense, Denmark
[6] ANU Medical School, The Australian National University, Canberra, Australian Capital Territory, Australia

Mutation of Dedicator of cytokinesis 8 (DOCK8) has previously been reported to provide resistance to the Th17 cell dependent EAE in mice. Contrary to expectation, we observed an elevation of Th17 cells in two different DOCK8 mutant mouse strains in the steady state. This was specific for Th17 cells with no change in Th1 or Th2 cell populations. In vitro Th cell differentiation assays revealed that the elevated Th17 cell population was not due to a T cell intrinsic differentiation bias. Challenging these mutant mice in the EAE model, we confirmed a resistance to this autoimmune disease with Th17 cells remaining elevated systemically while cellular infiltration in the CNS was reduced. Infiltrating T cells lost the bias toward Th17 cells indicating a relative reduction of Th17 cells in the CNS and a Th17 cell specific migration disadvantage. Adoptive transfers of Th1 and Th17 cells in EAE-affected mice further supported the Th17 cell-specific migration defect, however, DOCK8-deficient Th17 cells expressed normal Th17 cell-specific CCR6 levels and migrated toward chemokine gradients in transwell assays. This study shows that resistance to EAE in DOCK8 mutant mice is achieved despite a systemic Th17 bias.

Additional supporting information may be found online in the Supporting Information section at the end of the article.

Introduction

Inflammatory T helper 17 (Th17) cells are a CD4$^+$ T cell population that produce their namesake cytokine, IL-17 [1]. Over the last decade these cells have been associated with multiple diseases, including acute infections as well as chronic autoimmunity [2]. Th17 cells are particularly well described in the neurological inflammation model, EAE, a mouse model mimicking the

Correspondence: Dr. Anne Brüstle
e-mail: anne.bruestle@anu.edu.au

*These authors contributed equally to this work.

autoimmune component of MS [3]. Adoptive transfer of Th17 cells for example is sufficient to induce EAE [3, 4] and IL-17 production by Th17 cells is strongly linked to disease severity [4]. Further, deficiency in Th17 cell transcription factors, such as RORγt, STAT3, and IRF4 [5–7], and effector function, leads to a marked reduction in EAE pathology [8, 9].

Mutations in the gene for the guanine exchange factor, Dedicator of Cytokinesis 8 (DOCK8) have been associated with development of primary immunodeficiency in humans. The mutation results in a combined B and T cell immunodeficiency presenting with recurrent cutaneous viral infections, sinopulmonary infections, and risk of malignancy [10, 11]. The manifestations can all be cured by hematopoietic stem cell transplant, which is the preferred treatment modality due to the poor prognosis for these patients [12]. Immunodeficiency has also been observed in DOCK8 mutant mice, which demonstrate failure to sustain germinal center B cells [13], failure of T cell memory formation [14, 15], absent NKT cells [16], and failure of DC migration [17]. Studies of cell migration in skin have suggested that DOCK8 is important for maintenance of cell integrity when the cell undergoes shape changes during migration in tissues [18]. In humans, absence of DOCK8 leads to a T cell intrinsic bias toward Th2 cytokine production associated with elevated levels of IgE, at the expense of Th1 and Th17 cytokine production [19], but this hyper-IgE phenotype has not been seen in the mouse.

More recently, DOCK8 mutant mice have been shown to be protected from development of EAE [20]. Our study investigates the role of DOCK8 in Th17 cells, in particular, and the implications for the protective effect of mutation in DOCK8 recently observed in the EAE model.

Results

The functional absence of DOCK8 is protective in the EAE model

A point mutation of the murine *Dock8* gene has recently been shown to be protective in the EAE model, a mouse model for MS that is highly dependent on Th17 cells. Here, we analyzed two different mouse models of DOCK8 deficiency in this context, namely *Dock8$^{pri/pri}$* mice as used in the above mentioned study, which express full-length DOCK8 protein ([21], Supporting Information Fig. 1A) but in which substitution of a conserved serine for a proline at position 1827 abolishes the guanine exchange factor (GEF) activity for Cdc42 [22] and in addition, the *Dock8$^{E1886X/E1886X}$* mouse strain, which carries a mutation at position 1886 leading to a stop codon. These mice do not express DOCK8 protein ([21]; Supporting Information Fig. 1A). We found that both the DOCK8-GEF deficient mouse strain as well as the DOCK8-deficient *Dock8$^{E1886X/E1886X}$* strain were strongly protected from EAE (Fig. 1A and B). This protection was observed for all experimental animals as indicated by the breakdown of disease severity (Fig. 1C).

EAE disease is mainly mediated through Th17 cell induced immune cell infiltration into the CNS. Histological analysis of general cell infiltration (Fig. 1D, hematoxylin and eosin [H&E]), T cell infiltration (Fig. 1E, CD3), and astrocyte activation as an indicator of neurological inflammation (Fig. 1F, glial fibrillary acidic protein (GFAP)) revealed only minimal infiltration and inflammation in the absence of functional DOCK8. These findings were consistent with the recently published data using the *Dock8$^{pri/pri}$* mouse strain [20].

To investigate the nature of the cells that were able to infiltrate the CNS, lymphocytes were isolated from the brain and spinal cord using gradient centrifugation and the CD4$^+$ Th and CD8$^+$ cytotoxic lymphocyte (CTL) populations were quantified using flow cytometry, as a more accurate measure than immunohistochemistry. This revealed that the CD4$^+$ population was markedly reduced in DOCK8 mutant mice (Fig. 1G and H), while CD8$^+$ CTL infiltration was comparable between mutant and WT (Fig. 1I and J).

Elevated Th17 cells in the periphery of DOCK8 deficient mice were not due to T cell intrinsic effect

Functional Th17 cells are indispensable for the development of EAE and elevated Th17 cell responses have been described to aggravate disease [8]. Given the importance of Th17 cells in the development of EAE, we wanted to investigate whether there may be a deficiency of Th17 cells in these mouse strains, providing protection from EAE. Therefore, we investigated T cell subsets in the different DOCK8-deficient mouse strains. To do so, we first analyzed splenocytes from *Dock8$^{E1886X/E1886X}$* and *Dock8$^{pri/pri}$* mice immediately ex vivo for their expression of Th subset identifying cytokines. Contrary to expectations, both mouse strains showed a significant increase in the IL-17-producing Th17 cell population (Fig. 2A), excluding a deficiency of Th17 cells as a cause of the protection from EAE. This effect was only seen for the Th17 signature cytokine IL-17 and not for other T cell subset specific cytokines such as IFNγ (Th1) or IL-4 (Th2) (Fig. 2B and Supporting Information Fig. 2B).

To further investigate this unexpected finding, we checked whether the observed increase in Th17 cells may be due to a different distribution of CD4 T cells in the absence of DOCK8, or a T cell intrinsic bias in the formation of Th17 cells. To do this, we isolated naïve T cells from mutant mice and WT (*Dock8$^{+/+}$*) littermate controls of the two different DOCK8-deficient mouse strains (*Dock8$^{pri/pri}$* and *Dock8$^{E1886X/E1886X}$*) and differentiated them in vitro into Th1, Th2, and Th17 populations. The differentiation efficiency was measured by the production of the T cell subset-specific cytokines IFN-γ (Th1), IL-4 (Th2), and IL-17 (Th17). All differentiation conditions led to the production of the correct cytokines and no significant differences between DOCK8-deficient and sufficient T cell populations (Fig. 2C and Supporting Information Fig. 2C) were seen. This lack of an intrinsic bias was confirmed over a variety of different differentiation experiments (Fig. 2D).
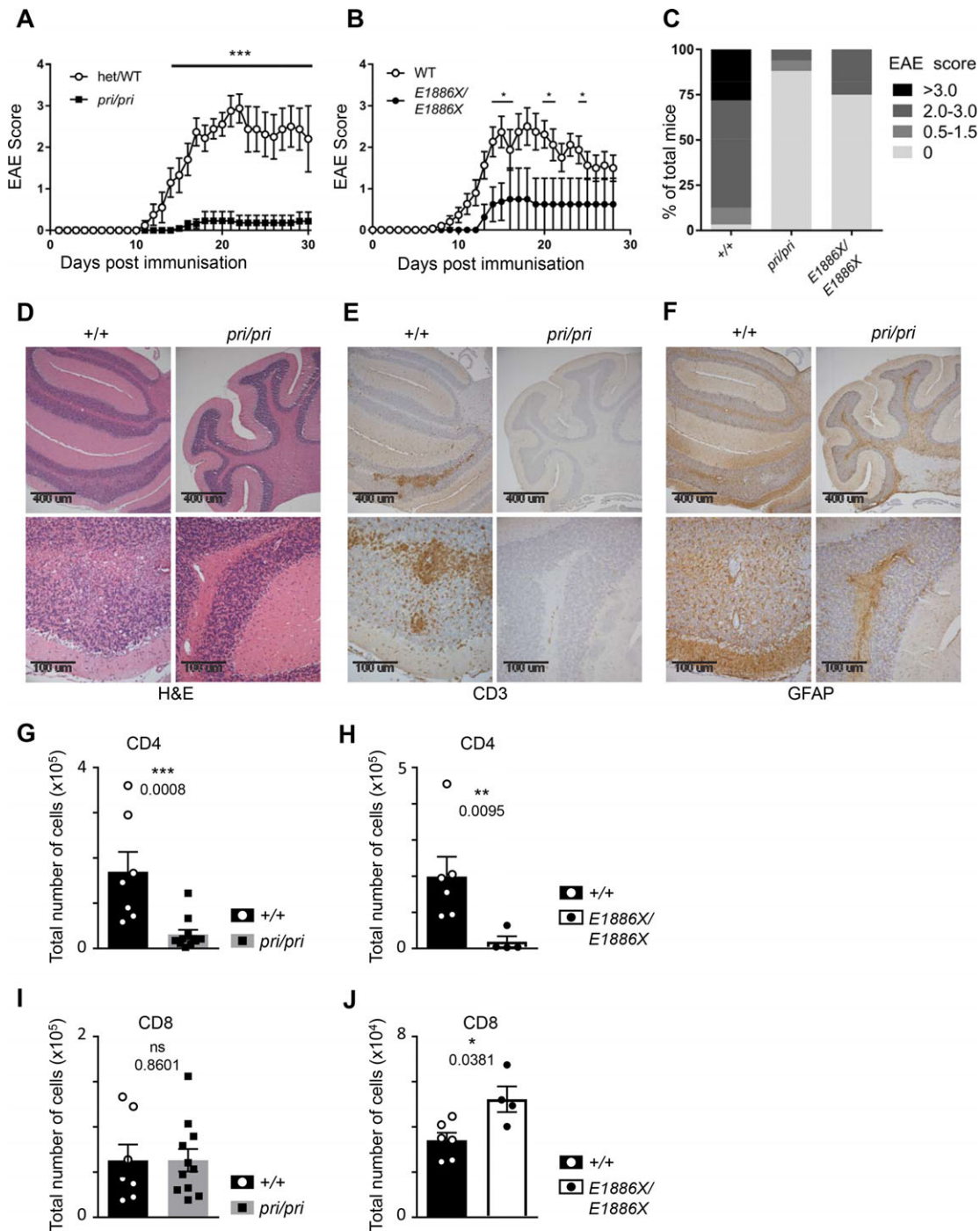
Figure 1. *Dock8$^{pri/pri}$* and *Dock8$^{E1886X/E1886X}$* mice are protected from EAE and show reduced CD4 T cell infiltration into the CNS. *Dock8$^{pri/pri}$*, *Dock8$^{E1886X/E1886X}$*, and littermate controls were immunized with MOG$_{35-55}$/CFA/PT to induce EAE. Mice were monitored daily over a period of 28–30 days post immunization for signs of disease. Mean clinical score of *Dock8$^{pri/pri}$* ($n = 22$), *Dock8$^{+/+}$* ($n = 17$; A), and *Dock8$^{E1886X/E1886X}$* ($n = 8$; B) mice and their littermate controls ($n = 15$) shown over the duration of the disease course $n > 8$. (C) Disease severity was calculated from the peak score reached by each mouse during the course of the disease, grouped into healthy (score 0) and mild (score 0.5–1.5), moderate (score 2.0–3.0) and severe (score > 3) disease. Data are from three independent pooled experiments. Shown are mean disease scores $\pm$ SEM. Significance was determined using the Holm–Sidak method. Sections were taken from brains of littermate *Dock8$^{+/+}$* and *Dock8$^{pri/pri}$* mice during the peak of disease (day 17) and stained with H&E (D) to identify total cellular infiltrates, anti-CD3 (E) for identification of T cell infiltrates and anti-GFAP (F) to examine neurological inflammation. Images shown are representative of 4–5 mice per group with data representative of two independent experiments. Scale bars 400/100 μm. The number of CNS (brain and spinal cord) infiltrating CD4 (G and H) and CD8 T cells (I and J) during the peak of disease (day 17–19 post immunization) were quantified for *Dock8$^{pri/pri}$* ($n = 11$) and littermate *Dock8$^{+/+}$* ($n = 7$) mice (G) and *Dock8$^{E1886X/E1886X}$* (H) mice ($n = 4$) and their littermate *Dock8$^{+/+}$* ($n = 6$) controls by flow cytometry. Dots represent individual mice with gating strategy described in Supporting Information Fig. 1B. Data are from a single experiment representative of three independent experiments. Bars show mean $\pm$ SEM. Significance was determined using unpaired Mann–Whitney U-test, ***$p < 0.001$; **$p < 0.01$; *$p > 0.05$; ns, not significant.

To further confirm that overly strong T cell receptor (TCR) stimulation was not masking subtle differences in differentiation, we performed differentiation experiments at different concentrations of CD3, as the amount of CD3 in the culture is a rough indicator of the TCR signal strength. While the overall production of the signature cytokine increased dose-dependently, no difference between DOCK8-deficient and $Dock8^{+/+}$ T cells was observed (Fig. 2E).

Th17 cells are also elevated in the periphery during EAE, but not in the CNS

To check whether the Th17 cells were also elevated during EAE, we analyzed splenocytes at the peak of disease (day 15–17 after EAE induction) by flow cytometry and found that they had elevated Th17 cells compared to EAE induced $Dock8^{+/+}$ mice (Fig. 3A). There have been reports of IL-10 producing non-pathogenic Th17 cells [23, 24], so we looked at IL-10 production by CD4$^+$ T cells at day 8 following EAE induction in spleen, and mesenteric and cervical lymph nodes. No IL-10 producing Th17 cells were detected. In fact, when looking at overall IL-10 production by CD4$^+$ T cells, we noted a decrease rather than increase in the $Dock8^{pri/pri}$ CD4$^+$ cells (Supporting Information Fig. 3C). We then determined the number of CNS (brain and spinal cord)-infiltrating CD4$^+$ cells producing only IL-17 (Th17), only IFN-γ (Th1), or both (Th1/17) at the peak of disease. Strikingly, the balance between IL-17-producing T cells, IFNγ-producing T cells, and those producing both cytokines was not altered (Fig. 3B and C) in $Dock8^{pri/pri}$ compared to $Dock8^{+/+}$mice. DOCK8 has been previously described as being important for cell migration [17, 18], particularly in complex environments. Our findings indicate a disproportionate decrease in the ratio of Th17 cells within the CNS, compared to systemically, in DOCK8 mutant mice. This raised the possibility of a T helper subset-specific migration defect in the absence of functional DOCK8.

Protection from EAE induction in DOCK8-deficiency has previously been connected to elevated levels of Leucine Rich Repeats and Calponin Homology Domain Containing 1 (LRCH1) [20]. Therefore, we wondered if the observed Th cell subset-specific difference in our two DOCK8-deficient mouse strains was linked to this phenomenon.

To investigate this, we measured protein levels of LRCH1 in $Dock8^{pri/pri}$ and $Dock8^{+/+}$ Th cells differentiated in vitro into Th1, Th2 and Th17 cells. LRCH1 was indeed differentially expressed in the tested Th cell subsets with very low expression in Th2 cells in $Dock8^{+/+}$ and $Dock8^{pri/pri}$, and higher levels of expression in Th1 and Th17 cells (Supporting Information Fig. 4). However, there was no difference in LRCH1 expression between Th1 and Th17 cells, nor any difference between $Dock8^{+/+}$ and $Dock8^{pri/pri}$ for these two subsets, indicating that differential expression of LRCH1 is not responsible for the diminished capacity of DOCK8 mutant Th17 cells to locate to the CNS.

DOCK8-deficient Th17 cells show normal chemotaxis and integrin expression but fail to cluster LFA-1

Th17 cells are recruited to the site of inflammation through the chemokine CCL20 and its corresponding receptor CCR6 [25]. In the context of EAE, CCR6 has been reported to regulate the migration of Th17 cells to various extents. Some reports show a strong reduction in EAE severity in the absence of CCR6 [26] while others only report a delay in disease onset [27, 28]. However, the number of Th17 cells infiltrating the CNS was severely reduced in all cases [26–28]. The expression level of CCR6 on Th17 cells might therefore provide an explanation for this subset-specific block in migration. We measured CCR6 expression on CD4$^+$ IL-17 expressing T cells from $Dock8^{pri/pri}$ and $Dock8^{E1886X/E1886X}$ mice and their corresponding littermate controls (Fig. 4A). DOCK8-deficiency did not reduce CCR6 expression. To test the chemokine sensing capability of DOCK8-deficient T cells, we performed transwell experiments. To do so, we mixed $Dock8^{pri/pri}$ and $Dock8^{+/+}$ T cells differentiated in vitro to the Th1 or Th17 cell linage in a 50:50 ratio and placed them on the top of the transwell chamber (Fig. 4B). CCL20, the ligand of CCR6, as well as IP-10, the ligand of CXCR3, the Th1 cell-specific chemokine receptor, were used [29]. Our data suggest that $Dock8^{pri/pri}$ T cells can migrate as effectively through these transwells as $Dock8^{+/+}$ cells. This effect was independent of the T cell subset and the presence or absence of the chemokine, and was consistent with previously published data [15].

Adhesion molecules such as integrins are also essential for the penetration of encephalitogenic T cells into the CNS [30]. We therefore explored the expression of α4β1 and LFA-1 on IFN-γ-producing (Th1) and IL-17-producing (Th17) splenocytes from DOCK8-deficient animals and littermate controls. In line with the published data, significantly more IFN-γ-producing splenocytes than IL-17-producing cells expressed α4β1 (Fig. 4C). This expression profile was independent of the presence of functional DOCK8. Interestingly, more Th1 cells also expressed LFA-1 (Fig. 4D). DOCK8 deficiency slightly increased the proportion of LFA-1 positive Th1 cells (Fig. 4D), however, when measured on splenocytes of EAE-induced mice on day 17, the levels of both integrins on Th1 cells were not different in the presence or absence of functional DOCK8 (Fig. 4E). In contrast, Th17 cells during peak EAE displayed significantly enhanced expression of both integrins in the absence of functional DOCK8 (Fig. 4E and F). This further underlines a Th17 cell specific effect in the absence of functional DOCK8.

Detection of expression of LFA-1 may not indicate functional capacity. Indeed, DOCK8 has been previously linked to LFA-1 dysfunction in T cells, with naïve CD8$^+$ T cells showing defective synaptic localization of LFA-1 upon recognition of cognate antigen presented by DCs [14] due to a failure of inside-out integrin activation in the absence of DOCK8. To investigate whether LFA-1 activation was also dysfunctional in CD4$^+$ cells, we investigated the localization of LFA-1 on Th1 and Th17 cells during their interaction with antigen presenting cells (APC). We differentiated $Dock8^{pri/pri}$ –OT-II transgenic T cells into Th1 and Th17 cells in vitro and co-cultured them with DCs presenting the OT-II-specific
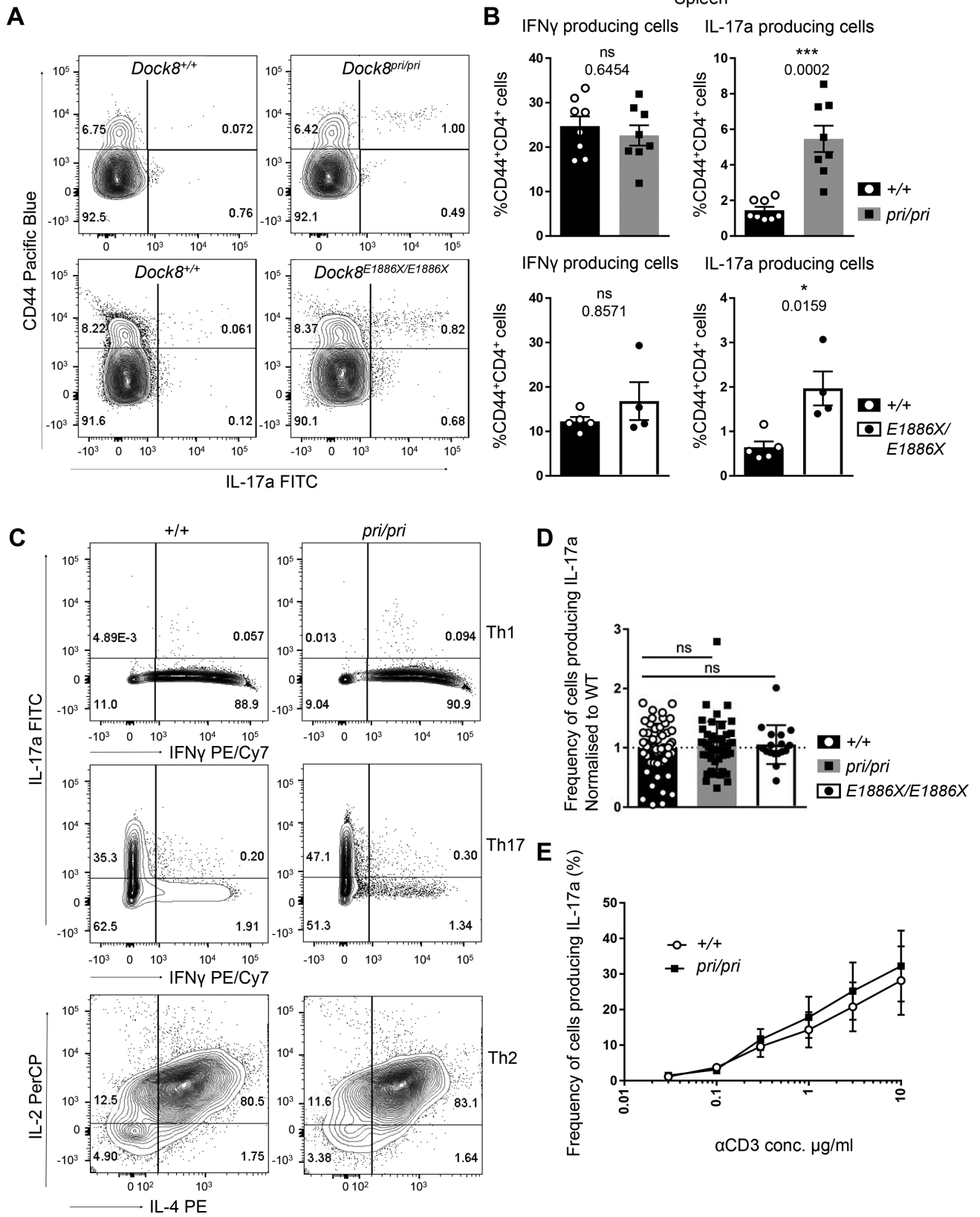
Figure 2. *Dock8* mutant mice have increased resting Th17 cell frequency. Splenocytes from naïve mice were isolated and stimulated for 4.5 h with PMA and ionomycin, and cytokine production was measured by flow cytometry using the gating strategy described in Supporting Information Fig. 1B. (A) Representative plots of intracellular cytokine staining from spleens of *Dock8^{pri/pri}*, *Dock8^{E1886X/E1886X}* mice, and litter mate controls stained for CD4, CD44, and IL-17a after ex vivo stimulation with PMA and ionomycin. (B) Splenic Th1 and Th17 cells as defined by their production of IFN-γ and IL-17, respectively, were quantified as frequency of activated CD4 T cells (CD4^+CD44^+ splenocytes) by flow cytometry. (A and B) $n = 4$–8 mice, data are from a single experiment representative of three to four individual experiments. Naïve T cells isolated from spleen and lymph nodes were differentiated into Th1, Th2, and Th17 cells by addition of specific polarizing cytokines and stimulation with anti-CD3 and anti-CD28. Cells were cultured for 5 days and then restimulated with PMA and ionomycin for 4.5 h. Differentiation of the cells from *Dock8^{+/+}* and *Dock8^{pri/pri}* mice was measured by intracellular cytokine staining, measuring production of key subset specific cytokines IL-17a, IFN-γ, and IL-4 pre-gated using the gating strategy described in Supporting Information Fig. 2A (C). The percentage of cells producing their signature cytokine was quantified and fold change in cytokine production compared to *Dock8^{+/+}* controls in the same experiment was determined to allow pooling of data (D). Differentiation of cells was then performed at different concentrations of anti-CD3 to mimic differential TCR stimulation alongside standard quantities of cytokines. Percentages of cells in the Th17 condition producing IL-17 were quantified across concentrations of anti-CD3 (E) with $n = 3$ mice per genotype per experiment. Data are from a single experiment representative of two independent experiments. Bars show mean ± SEM. Error bars show SEM. Significance was determined using unpaired Mann–Whitney U-test, ***$p < 0.001$; **$p < 0.01$; *$p > 0.05$; ns, not significant. All dot plots depicted are representative of a minimum of three independent experiments.

OVA peptide. Imaging of the immunological synapse of both Th1 and Th17 cell populations using T cell synapse-specific markers indicated a defect in the polarization of actin and, more strikingly, LFA-1, to the immunological synapse in both DOCK8 mutant T cell populations (Fig. 5A–C). These data suggested that both Th1 and Th17 cells from DOCK8 mutant mice form a dysfunctional synapse with APCs, as has previously been observed for CD8^+ T cells [14], and may not be able to activate the surface LFA-1.

DOCK8-deficient Th17 cells have diminished capacity to locate to the CNS

To functionally investigate the migration of Th cell subsets in the complex system of EAE, we performed adoptive transfer experiments. In brief, we differentiated naïve CD4^+ T cells of *Dock8^{pri/pri}* and *Dock8^{+/+}* mice in vitro into Th1 and Th17 subsets. Differentially labeled cells were then transferred into recipient mice at a 50:50 ratio at day 11 after EAE induction (Fig. 5D).

Cell infiltration into multiple organs was then measured 16 h later by flow cytometry. Interestingly, no change in ratio was observed in any organ tested except for the CNS (Fig. 5E). Here, we observed a significantly higher recovery of *Dock8^{+/+}* Th17 cells compared to DOCK8-deficient Th17 cells and we observed the opposite effect in the Th1 cell recovery ratio (Fig. 5F). In some complex environments, DOCK8 mutant cells are known to undergo cytothripsis or cell death. Analysis of the recovered cells in the CNS did not indicate a higher rate of cellular death in the DOCK8 mutant mice (Supporting Information Fig. 6B). This data supported a Th17 cell subset-specific migration defect in the absence of functional DOCK8.

Discussion

In this paper, we present our novel findings that in the steady state DOCK8-deficient mouse strains have elevated Th17 cells, but the protection from EAE observed in these mice is likely due
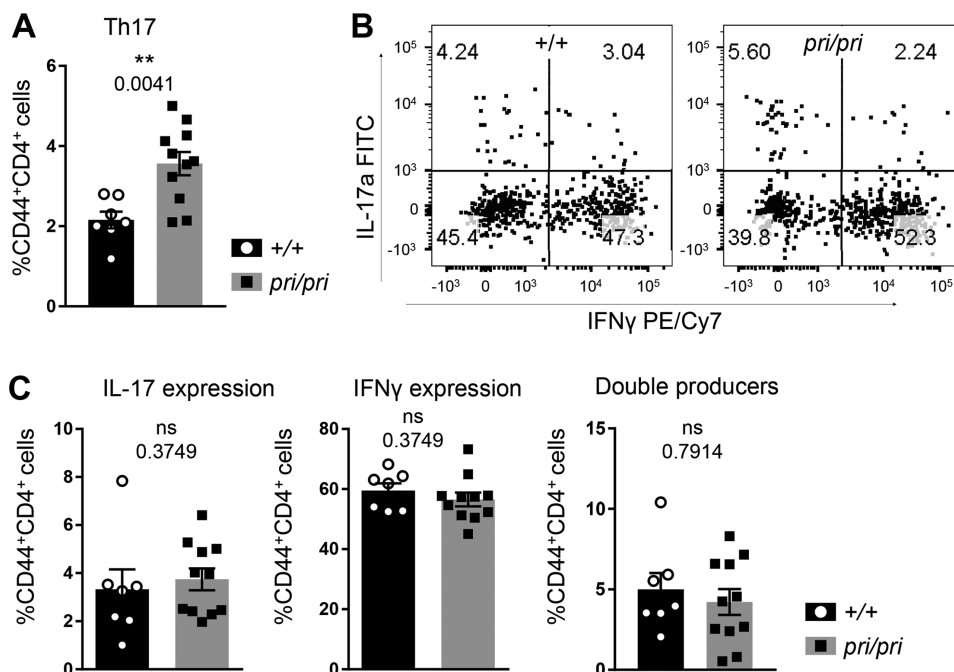
Figure 3. Dock8 deficient Th17 cells accumulate in the spleen during EAE. Cells collected from *Dock8^{pri/pri}* ($n = 11$) and littermate control *Dock8^{+/+}* ($n = 7$) mice during the peak phase of EAE (day 15–17) were restimulated ex vivo with PMA and ionomycin for 4.5 h in the presence of a Golgi inhibitor. Cytokine production was measured by intracellular cytokine staining using the gating strategy described in Supporting Information Fig. 1B and Th17 cells, as defined by IL-17 production, were quantified from the splenocytes (A) and CNS (brain and spinal cord) infiltrating lymphocytes (B and C) of the mice using flow cytometry. Dots represent individual mice, data are from a single experiment representative of two independent experiments. Bars show mean ± SEM. Significance was determined using unpaired Mann–Whitney U-test, ***$p < 0.001$; **$p < 0.01$; *$p > 0.05$; ns, not significant.
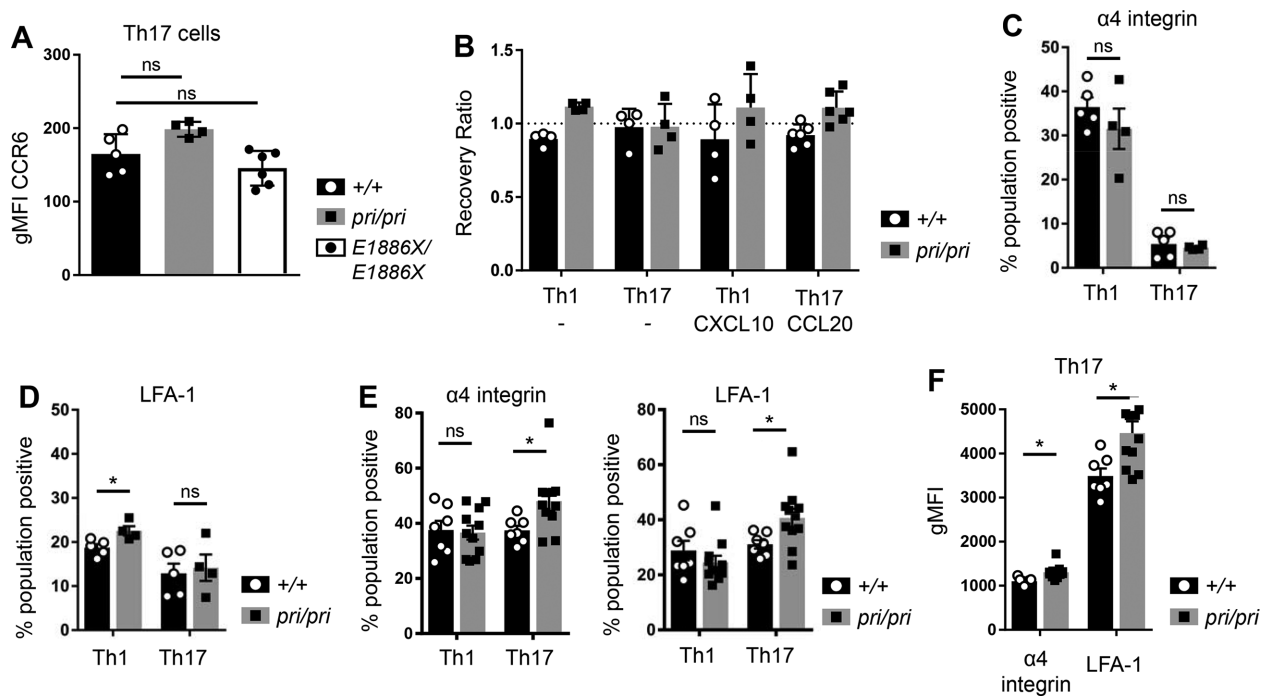
Figure 4. *Dock8* mutant cells express factors necessary for migration and respond to chemokine signals. (A) Splenocytes from naïve *Dock8$^{pri/pri}$* ($n = 4$), *Dock8$^{E1886X/E1886X}$* ($n = 6$), and littermate control mice ($n = 5$) were examined for their expression CCR6 on Th17 cells (CD4$^+$CD44$^+$IL-17$^+$) by flow cytometry using the gating strategy described in Supporting Information Fig. 1B. Dots represent individual mice representative of two experiments. Data are from a single experiment, representative of two independent experiments. Bars show mean ± SEM. Significance was calculated using one-way ANOVA. Naïve *Dock8$^{pri/pri}$* and littermate control T cells were differentiated in vitro for 3 days into Th1 and Th17 cells. Differentiated cells were assessed for their ability to migrate across an 8 μM pore transwell in response to media alone, or to their subset-specific chemokine CXCL10 (IP-10) or CCL20 for Th1 and Th17 cells, respectively. (B) Migration was measured as the recovery ratio cells compared to input. Dots represent biological repeats pooled from three independent experiments with four to six mice per group. Significance was calculated using a two-way ANOVA with Sidak's multiple comparison. Bars show the mean ± SEM. Integrin expression was measured by analyzing the percentage of Th1 (CD4$^+$CD44$^+$IFN-γ^+) and Th17 (CD4$^+$CD44$^+$IL-17$^+$) cells from naïve *Dock8$^{pri/pri}$* ($n = 4$) and *Dock8$^{+/+}$* ($n = 5$) mice expressing α4 integrin (C) and LFA-1 (D) using the gating strategy described in Supporting Information Fig. 5. This was compared to splenocytes from *Dock8$^{pri/pri}$* ($n = 11$) and littermate control mice ($n = 7$) collected during the peak phase of EAE (day 17 post immunization; E). (F) Per cell expression of α4 integrin and LFA-1 on Th17 splenocytes collected during the peak of EAE was calculated using the geometric mean of fluorescence intensity for each antibody. Dots represent individual mice, data are from a single experiment representative of two independent experiments, Bars show mean ± SEM. Significance was determined using unpaired Mann–Whitney *U*-test, ***$p < 0.001$; **$p < 0.01$; *$p > 0.05$; ns, not significant.

to a specific decrease in Th17 infiltration of the CNS (despite the presence of elevated levels of these cells systemically).

The finding of elevated Th17 cell in the DOCK8-deficient mice differs from the findings in patients with DOCK8 immunodeficiency, where both Tangye et al. [19] and Keles et al. [31] have shown a decreased number of Th17 cells in patients—one by direct flow cytometric measurement, the other by in vitro differentiation and measurement of signature transcription factors. This discordance may be due to an intrinsic difference between mice and humans, like the Th2 bias seen in patients with DOCK8 immunodeficiency [19] that is not mirrored in the mutant mice, or may be due to the differential immune activation between mice housed in pathogen free conditions and patients who present with multiple concurrent viral infections and are likely on a number of medications.

Th17 cells are transcriptionally, and in their effector function, closely related to RORγT$^+$ innate lymphoid cells (ILC3) [32]. Interestingly, Singh et al. [33] have shown a deficiency in ILC3s in the *Dock8$^{pri/pri}$* mouse strain partially due to a decrease in STAT3 phosphorylation and consequently signaling. However, our in vitro

cell differentiation of Th17 cells (dependent on STAT3 phosphorylation [6]) did not require functional DOCK8, supporting a role for normal function of STAT3 under these circumstances. This not only highlights the differences between the generation of Th17 cells and ILC3s, but suggests a differential role for DOCK8 that is not dependent on cytokine signaling, transcriptional regulation, or effector cytokine production.

Our adoptive transfer experiments clearly show a DOCK8-specific defect in migration that is specific to the Th17 cell population, but does not appear to be due to defective general chemotaxis of this T cell subset. The elevated Th17 cell population is exacerbated in the spleen of EAE-induced animals, but not in the CNS, suggesting that one of the T cell extrinsic reasons for the Th17 elevation is a failure of equal distribution of the cells. DOCK8-deficient cells are known to have migration defects when passing through tight structures [18]. However, in our model, CD8$^+$ and, even more strikingly, Th1 cells have no defect entering the brain through the blood–brain barrier, supporting the possibility of a Th17 cell-specific defect, rather than a general cellular loss.

Xu et al. [20] proposed that protection against EAE, afforded by the presence of mutations in DOCK8, is due to (lack of) interaction with LRCH1 that usually restrains Cdc42 activation due to DOCK8. They proposed that LRCH1 binds to the DHR2 domain of DOCK8 to inhibit its interaction with Cdc42, and that this interaction is decreased by the phosphorylation of specific serine residues in the C terminus by PKCα. Having two different mouse strains—one with full length DOCK8, but with a defective DHR2 domain but intact terminal serine residues, and one in which no protein is expressed—allowed us to compare LRCH1 expression in the presence or absence of DOCK8 expression, and we found while there were differences in LRCH1 expression between T helper subsets, the expression was not affected by the presence or absence of DOCK8 expression, and there was no differential expression of LRCH1 in Th17 cells between DOCK8 mutant and WT cells indicating that this mechanism was unlikely to be responsible for the differential migration we observed in the Th subsets.

We further show for the first time, that both Th1 and Th17 CD4+ T cells have impaired immunological synapse formation in the absence of functional DOCK8, as well as a failure of clustering of LFA-1, indicating a failure of the inside out integrin activation required for LFA-1 function. Blocking of α4 integrins has been shown to affect Th1 cells, but not Th17 cell infiltration into the CNS, suggesting that LFA-1 is the most functional integrin on Th17 cells [34]. We therefore propose that one possibility to explain our findings is that the Th17 cell migration defect described is due to a higher reliance of Th17 cells on the DOCK8-dependent arrangement of adhesion molecules, such as LFA-1. Interestingly, we observed elevated levels of adhesion molecules on Th17 cells, particularly during inflammation, and this effect is significantly enhanced in the absence of functional DOCK8. This strong induction across all tested molecules may be a sign of a compensatory effect in DOCK8-deficient Th17 cells to overcome the restrictions in adhesion molecule rearrangement.

Concluding remarks

Our studies reveal the novel finding that DOCK8 mutant mice, in contrast to the findings in humans, have elevated Th17 cells. Despite this, they do not get exaggerated EAE but appear protected due to a Th17 specific migration defect to the CNS.

Materials and methods

Mice

The *Dock8*[pri/pri] and *Dock8*[E1886X/E1886X] mice on the C57BL/6 background were generated by ENU mutagenesis, as previously described [13, 21]. *Dock8*[pri/pri] mice (substrain C57BL/6J-Anu) have a T to C substitution that changes aa 1827 to a proline residue. Full length DOCK8 protein is expressed on Western Blot but this strain has the same phenotype as a knock out strain. *Dock8*[E1886X/E1886X] (substrain C57BL/6Crl-Anu) have a G to T sub-

stitution introducing a premature stop codon at aa 1886 and this results in no expression of DOCK8 protein [21]. All animals were backcrossed onto the indicated C57BL/6 background. Sex matched littermate controls were used for all experiments. Mice were housed in a pathogen free facility and all procedures were approved by the Australian National University Animal Ethics and Experimentation Committee.

Flow cytometry

The following antibodies were used: CCR6 PE (Miltenyi, REA277); CD3 PerCP Cy5.5 (Biolegend, 17A2); CD4 APC (BD Pharmingen, RM4-5) and A700 (Biolegend, RM4-5); CD44 Pacfic Blue (Biolegend, IM7); CD45.1 A700 (Biolegend, A20), CD45.2 APC (eBioscience, 104); CD62L APC-CY7 (Thermofisher, MEL-14); CD8-BV605 (BD Biosciences, 53–6.7); CD11a PE (Biolegend, 2D7); CD11b PerCP Cy5.5 (Biolegend, M1/70); IFN-γ (eBioscience, XMG1.2); IL-17a FITC (Biolegend, TC11-18H), IL-17a BV605 (Biolegend, TC11-18H); IL-4 PE (Miltenyi, BVD4-1D11); and Live Dead Fixable Viability Dye e780 (eBioscience). Flow cytometry was performed using an LSRII machine (BD Biosciences) and analyzed using FlowJo 10.2 software (Tree Star). Authors adhered to the *European Journal of Immunology* guidelines for the use of flow cytometry and cell sorting in immunological studies [38]. All gating strategies are shown in Supporting Information figures and referred to in the appropriate figure legends.

CD4 T cell purification

Naïve CD4+ T cells were isolated from spleens and lymph nodes of mice by magnetic- and fluorescence-activated cell sorting (FACS). In short, naïve cells were isolated either by using the CD4CD62L naïve isolation kit (Miltenyi) or by using a combination of the CD4 (L3T4) isolation kit (Miltenyi) and subsequent FACS sorting of naïve cells based on CD4, CD62L, and CD44 expression using the BD FACS Aria II (BD Biosciences). Purity of naïve cells was verified by flow cytometry to be above 90% in all cases.

T cell differentiation

Isolated naïve T cells were stimulated for 72 h using 3 μg/mL of plate bound anti-CD3 in combination with 2 μg/mL anti-CD28 (both from BioXcell). Cells were differentiated into Th1 cells by the addition of 5 ng/mL IL-2 and 4 ng/mL IL-12 (both from Miltenyi) in combination with 2.5 μg/mL anti-IL-4 (BioXcell). Cells were differentiated into Th17 cells through addition of 30 ng/mL IL-6, 0.5 ng/mL TGF-β (both from Miltenyi) alongside 2.5 μg/mL anti-IL-4 and 2.5 μg/mL anti-IFN-γ (BioXcell).

Th2 cells were differentiated by the addition of 10 ng/mL IL-4 (Miltenyi) in combination with 5 μg/mL anti-IFN-γ. After 72 h, cells were split and incubated with fresh media supplemented with IL-2 for a further 24 h.

Cells were cultured in complete IMDM (Thermofisher, with 10% FCS, Penicillin, streptomycin, glutamine, and β-mercaptoethanol).
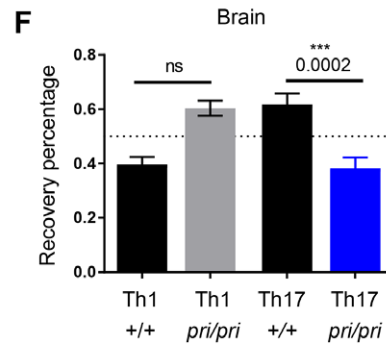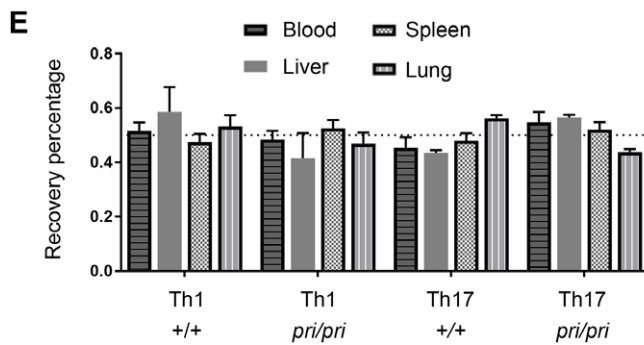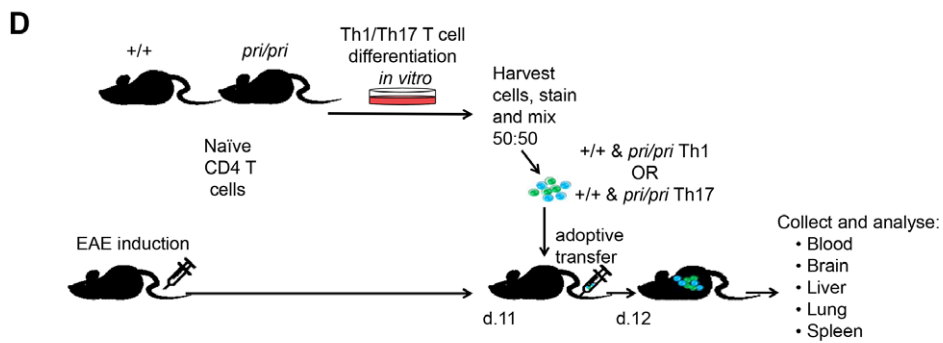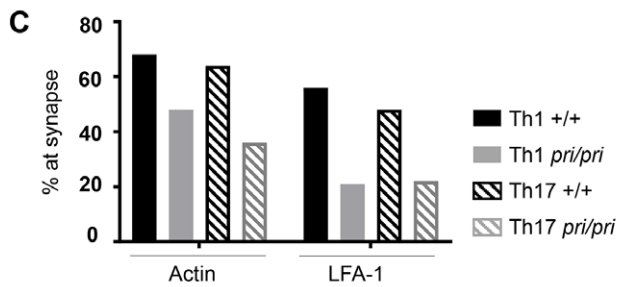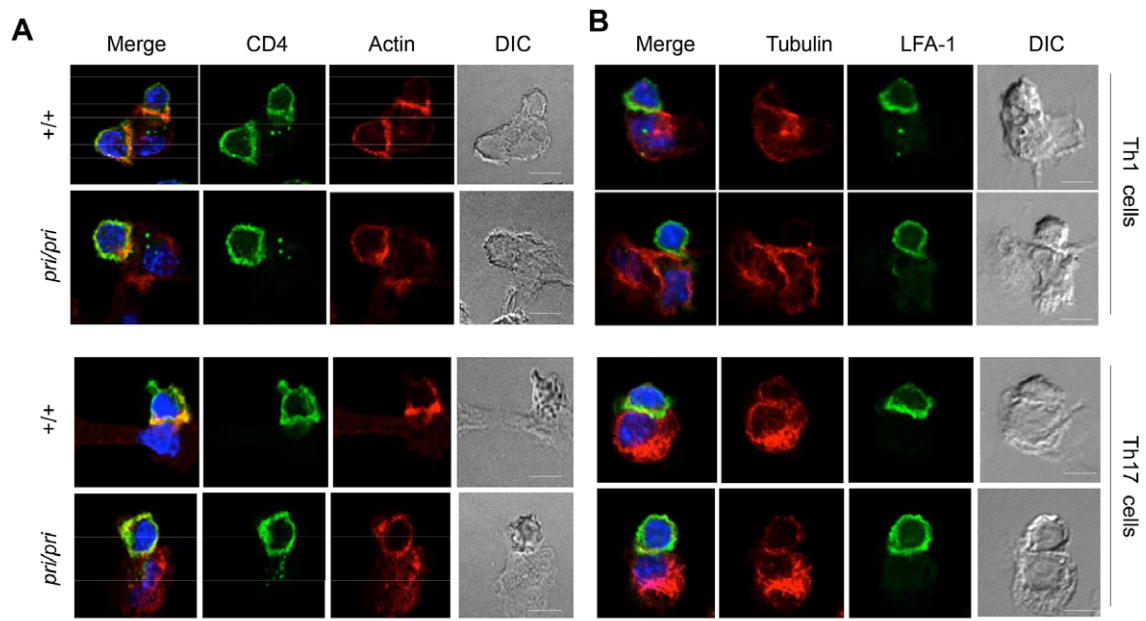
EAE induction

EAE was induced in 8–12 wk old mice by subcutaneous immunization with 115 μg per mouse myelin oligodendrocyte gp (MOG35-55 genscript) in Complete Freund's Adjuvant (Sigma) on day 1. Pertussis toxin (300 ng per mouse; List Biological Laboratories) in PBS was injected i.p. on days 0 and 2. Mice were monitored daily for signs of disease and were scored on a scale of 0–5 based on physical manifestations of disease. Mice were scored as follows: 0, clinically normal; 1, flaccid tail and/or ataxia; 2, hind limb weakness; 3, hind limb paralysis; 4, hind and front limb paralysis; and 5, moribund.

Isolation of lymphocytes from tissues of immunized mice

On day 15–17 after induction of EAE, mice were euthanized with CO_2, and their circulatory systems perfused with 10 mL PBS through the heart. Brains and spinal cords were collected into PBS supplemented with 1% FCS and subsequently digested for 30 min at 37°C in RPMI containing 50 μg/mL collagenase (Sigma) and 10 μg/mL DNAse I (Roche). Lymphocytes were collected after centrifugation through a Percoll (Sigma) bilayer (40 and 70%) and were then washed twice with PBS supplemented with 1% FCS before staining and further analysis. Cells were isolated from livers of mice using the same method. Lungs collected from mice were digested similarly, red blood cells lysed, and remaining lymphocytes washed with PBS.

Histology and Immunohistochemistry

Histological sections of brains were obtained as previously described [9, 35]. H&E staining and immunohistochemical (IHC) analyses were performed using standard laboratory procedures as described previously [9].

Intracellular cytokine staining

Lymphocytes collected from blood, spleen, lymph nodes, brain or from culture were washed with 1% FCS in PBS and stained for surface markers for 30 min. Cells were then washed with PBS and stimulated for 4 h 30 min with 50 nM PMA (Sigma–Aldrich) and 750 nM Ionomycin (Sigma–Aldrich) in addition to Golgi Stop (1:1000; BD Bioscience). Stimulated cells were then washed with PBS and incubated with Fixable Viability Dye e780 (1:1000; eBioscience) for 20 min. Fixation, permeabilization, and intracellular cytokine staining was performed using the FoxP3 staining kit (eBioscience), as described by the manufacturer.

Cell transfer for in vivo migration assay

Cells were harvested after 5 days in T cell differentiation culture and washed once with RPMI supplemented with 10% FCS. Cells were then resuspended in this media and stained using 10 μM CTV (Invitrogen) or CFSE (Sigma) dyes. Cells were washed twice with sterile PBS, counted, and mixed so as to create 50:50 aliquots of cells from different genotypes. Approximately 1×10^6 cells in 200 μL PBS was injected i.v. into each mouse. Mice were culled after approximately 18 h.

Transwell migration assays

Cells were harvested after 5 days in T cell differentiation culture and washed once with IMDM supplemented with 10% FCS. Either $Dock8^{+/+}$ or $Dock8^{pri/pri}$ cells were then resuspended in 1 mL of media and stained with 10 μM CTV for 5 min at room temperature. Cells were washed twice with media, counted, and combined in a 50:50 ratio with unstained cells of the opposite genotype. Cells were then placed into the top of a transwell (8 μm pore, Sigma) over a well containing either 1 μg/mL CCL20 (R&D Systems) or 500 ng/mL IP-10 (Peprotech). Cells were then incubated for 2 h at 37°C and migrated cells collected from the bottom of the well. Cell migration was analyzed by flow cytometry and normalized to the starting cell ratio as verified by flow cytometry.

Immunofluorescence and confocal microscopy

For immunofluorescence staining, $Dock8^{+/+}$ or $Dock8^{pri/pri}$ CD4^{+} OT-II T cells were co-cultured with Ovalbumin peptide[329-337]-

Figure 5. DOCK8 deficiency impairs actin and LFA-1 localization to the immunological synapse and causes Th17 cell specific CNS migration defects. $Dock8^{+/+}$ or $Dock8^{pri/pri}$ CD4^{+} (OT-II) Th1 or Th17 T cells were co-cultured with peptide-pulsed DCs for 1 h, then fixed and stained for the protein of interest. (A) T cell–DC conjugates stained for CD4 (green) and actin (red). (B) T cell–DC conjugates stained for tubulin (red) and LFA-1 (green). Blue, DAPI in the merged image. Scale bar 10 μm. (C) Quantitation of the percentage of cells with either actin or LFA-1 polarized to the T cell–DC interface in each condition ($n = 25$–65 cells) pooled from two independent experiments with one biological replicate in each. (D) Congenically marked naïve T cells isolated from spleen and lymph nodes of $Dock8^{pri/pri}$ mice and littermate controls were differentiated into Th1 and Th17 cells for 3 days by addition of specific polarizing cytokines and stimulation with anti-CD3 and CD-28. Differentiated Th1 and Th17 cells were harvested and stained using CTV/CFSE and genotypes mixed in a 50:50 ratio. Cell mixes were then injected i.v. into mice (expressing a different congenic marker) that had been immunized 11 days prior with MOG_{35-55}/CFA/PT to induce EAE. (E) Migration of transferred cells to peripheral organs (E) and the brain (F) was measured by analyzing the recovery percentage of labeled in vitro differentiated Th1 and Th17 $Dock8^{+/+}$ and $Dock8^{pri/pri}$ cells 16 h after adoptive transfer ($n = 3$–9 mice pool from two independent experiments) using the gating strategy described in Supporting Information Fig. 6A. Three donor mice per genotype per experiment were used with two to five recipient mice per cell type per experiment. Data are from a single experiment, representative of two independent experiments. Bars show mean ± SEM. Significance was determined using an unpaired Mann–Whitney U-test, ***$p < 0.001$; **$p < 0.01$; *$p > 0.05$; ns, not significant.

pulsed BM–derived DCs in chamber slides for 1 h. The cell conjugates formed were then fixed and permeabilized for imaging as previously described [36]. Cell conjugates were stained for the proteins of interest using the following primary antibodies: anti–LFA-1 (BD Biosciences), anti-CD8 (BD Biosciences), actin/phalloidin rhodamine (Invitrogen), and mouse tubulin (Rocklands) or rabbit tubulin (Sigma–Aldrich), followed by secondary antibodies (anti-rat and anti-rabbit Alexa Fluor 488 and anti-mouse and anti-rabbit Alexa Fluor 546). The cells were mounted in ProLong Gold antifade reagent with DAPI (Invitrogen). Cells were imaged using a confocal microscope (Fluoview FV1000; Olympus) equipped with a 12.9-mW 488-nm multi-ion argon laser, a 1-mW 543-nm multi-ion green HeNe laser, and an 11-mW 633-nm red HeNe laser. All images were captured using a PlanApoN 60 Å-oil immersion objective (NA = 1.42). The images were subsequently processed using the Olympus Micro FV10-ASW program. To acquire images in which an immune synapse was formed, conjugates of single T cells rounded and in close contact with the interface of a DC were chosen. Blinded scoring of the images was used as a means for quantifying the localization of proteins of interest. An integer score was given from 3 (very polarized to the T cell-DC interface), 2 (partially polarized to the T cell-DC interface), to 1 (not polarized, spread around the T cell surface). Only cells that scored 3 are plotted in Fig. 5C, for >25 cells per condition.

Immunoblotting and antibodies

Immunoblotting was performed, as described previously [37], and T cells were differentiated for 72 h into Th1, Th2, and Th17 cells, as described above. Antibodies used for immunoblotting were as follows: anti-LRCH1 (Abcam) anti-DOCK8 (Sigma), anti-actin (Sigma–Aldrich).

Statistical analysis

Statistical data analysis was performed using GraphPad Prism 7 software. When comparing two variables, a Mann–Whitney U-test was used to avoid the assumption of normal distribution. When comparing more than two groups, a one-way ANOVA was used. For multi-variant analysis, two-way ANOVA with Sidak's multiple comparison test was used. For all tests, $p < 0.05$ was considered significant with p values reported as follows; ***$p < 0.001$; **$p < 0.01$; *$p > 0.05$; ns, not significant.

Conflict of Interest: The authors declare no commercial or financial conflict of interest.

References

1 **Korn, T., Bettelli, E., Oukka, M. and Kuchroo, V. K.,** IL-17 and Th17 Cells. *Annu. Rev. Immunol.* 2009. **27**: 485–517.

2 **Singh, R. P., Hasan, S., Sharma, S., Nagra, S., Yamaguchi, D. T., Wong, D. T., Hahn, B. H. et al.,** Th17 cells in inflammation and autoimmunity. *Autoimmun. Rev.* 2014. **13**: 1174–1181.

3 **Langrish, C. L., Chen, Y., Blumenschein, W. M., Mattson, J., Basham, B., Sedgwick, J. D., McClanahan, T. et al.,** IL-23 drives a pathogenic T cell population that induces autoimmune inflammation. *J. Exp. Med.* 2005. **201**: 233–240.

4 **Bettelli, E., Carrier, Y., Gao, W., Korn, T., Strom, T. B., Oukka, M., Weiner, H. L. et al.,** Reciprocal developmental pathways for the generation of pathogenic effector TH17 and regulatory T cells. *Nature* 2006. **441**: 235–238.

5 **Ivanov, II, McKenzie, B. S., Zhou, L., Tadokoro, C. E., Lepelley, A., Lafaille, J. J., Cua, D. J. et al.,** The orphan nuclear receptor RORgammat directs the differentiation program of proinflammatory IL-17+ T helper cells. *Cell* 2006. **126**: 1121–1133.

6 **Harris, T. J., Grosso, J. F., Yen, H. R., Xin, H., Kortylewski, M., Albesiano, E., Hipkiss, E. L. et al.,** Cutting edge: An in vivo requirement for STAT3 signaling in TH17 development and TH17-dependent autoimmunity. *J. Immunol.* 2007. **179**: 4313–4317.

7 **Brustle, A., Heink, S., Huber, M., Rosenplanter, C., Stadelmann, C., Yu, P., Arpaia, E. et al.,** The development of inflammatory T(H)-17 cells requires interferon-regulatory factor 4. *Nat. Immunol.* 2007. **8**: 958–966.

8 **Jeltsch, K. M., Hu, D., Brenner, S., Zoller, J., Heinz, G. A., Nagel, D., Vogel, K. U., et al.,** Cleavage of roquin and regnase-1 by the paracaspase MALT1 releases their cooperatively repressed targets to promote T(H)17 differentiation. *Nat. Immunol.* 2014. **15**: 1079–1089.

9 **Brustle, A., Brenner, D., Knobbe, C. B., Lang, P. A., Virtanen, C., Hershenfield, B. M., Reardon, C. et al.,** The NF-kappaB regulator MALT1 determines the encephalitogenic potential of Th17 cells. *J. Clin. Invest.* 2012. **122**: 4698–4709.

10 **Zhang, Q., Davis, J. C., Lamborn, I. T., Freeman, A. F., Jing, H., Favreau, A. J., Matthews, H. F. et al.,** Combined immunodeficiency associated with DOCK8 mutations. *N. Engl. J. Med.* 2009. **361**: 2046–2055.

11 **Engelhardt, K. R., McGhee, S., Winkler, S., Sassi, A., Woellner, C., Lopez-Herrera, G., Chen, A. et al.,** Large deletions and point mutations involving the dedicator of cytokinesis 8 (DOCK8) in the autosomal-recessive form of hyper-IgE syndrome. *J. Allergy Clin. Immunol.* 2009. **124**: 1289–1302 e1284.

12 **Aydin, S. E., Kilic, S. S., Aytekin, C., Kumar, A., Porras, O., Kainulainen, L., Kostyuchenko, L. et al.**, and inborn errors working party of, E., DOCK8 deficiency: clinical and immunological phenotype and treatment options—a review of 136 patients. *J. Clin. Immunol.* 2015. **35**: 189–198.

13 **Randall, K. L., Lambe, T., Johnson, A. L., Treanor, B., Kucharska, E., Domaschenz, H., Whittle, B. et al.**, Dock8 mutations cripple B cell immunological synapses, germinal centers and long-lived antibody production. *Nat. Immunol.* 2009. **10**: 1283–1291.

14 **Randall, K. L., Chan, S. S., Ma, C. S., Fung, I., Mei, Y., Yabas, M., Tan, A. et al.**, DOCK8 deficiency impairs CD8 T cell survival and function in humans and mice. *J. Exp. Med.* 2011. **208**: 2305–2320.

15 **Lambe, T., Crawford, G., Johnson, A. L., Crockford, T. L., Bouriez-Jones, T., Smyth, A. M., Pham, T. H. et al.**, DOCK8 is essential for T-cell survival and the maintenance of CD8⁺ T-cell memory. *Eur. J. Immunol.* 2011. **41**: 3423–3435.

16 **Crawford, G., Enders, A., Gileadi, U., Stankovic, S., Zhang, Q., Lambe, T., Crockford, T. L. et al.**, DOCK8 is critical for the survival and function of NKT cells. *Blood* 2013. **122**: 2052–2061.

17 **Harada, Y., Tanaka, Y., Terasawa, M., Pieczyk, M., Habiro, K., Katakai, T., Hanawa-Suetsugu, K. et al.**, DOCK8 is a Cdc42 activator critical for interstitial dendritic cell migration during immune responses. *Blood* 2012. **119**: 4451–4461.

18 **Zhang, Q., Dove, C. G., Hor, J. L., Murdock, H. M., Strauss-Albee, D. M., Garcia, J. A., Mandl, J. N. et al.**, DOCK8 regulates lymphocyte shape integrity for skin antiviral immunity. *J. Exp. Med.* 2014. **211**: 2549–2566.

19 **Tangye, S. G., Pillay, B., Randall, K. L., Avery, D. T., Phan, T. G., Gray, P., Ziegler, J. B. et al.**, Dedicator of cytokinesis 8-deficient CD4⁺ T cells are biased to a TH2 effector fate at the expense of TH1 and TH17 cells. *J. Allergy Clin. Immunol.* 2017. **139**: 933–949.

20 **Xu, X., Han, L., Zhao, G., Xue, S., Gao, Y., Xiao, J., Zhang, S. et al.**, LRCH1 interferes with DOCK8-Cdc42-induced T cell migration and ameliorates experimental autoimmune encephalomyelitis. *J. Exp. Med.* 2017. **214**: 209–226.

21 **Flesch, I. E., Randall, K. L., Hollett, N. A., Di Law, H., Miosge, L. A., Sontani, Y., Goodnow, C. C. et al.**, Delayed control of herpes simplex virus infection and impaired CD4(+) T-cell migration to the skin in mouse models of DOCK8 deficiency. *Immunol. Cell Biol.* 2015. **93**: 517–521.

22 **Janssen, E., Tohme, M., Hedayat, M., Leick, M., Kumari, S., Ramesh, N., Massaad, M. J. et al.**, A DOCK8-WIP-WASp complex links T cell receptors to the actin cytoskeleton. *J. Clin. Invest.* 2016. **126**: 3837–3851.

23 **Heink, S., Yogev, N., Garbers, C., Herwerth, M., Aly, L., Gasperi, C., Husterer, V. et al.**, Trans-presentation of IL-6 by dendritic cells is required for the priming of pathogenic TH17 cells. *Nat. Immunol.* 2017. **18**: 74–85.

24 **Lee, Y., Awasthi, A., Yosef, N., Quintana, F. J., Xiao, S., Peters, A., Wu, C. et al.**, Induction and molecular signature of pathogenic TH17 cells. *Nat. Immunol.* 2012. **13**: 991–999.

25 **Hirota, K., Yoshitomi, H., Hashimoto, M., Maeda, S., Teradaira, S., Sugimoto, N., Yamaguchi, T. et al.**, Preferential recruitment of CCR6-expressing Th17 cells to inflamed joints via CCL20 in rheumatoid arthritis and its animal model. *J. Exp. Med.* 2007. **204**: 2803–2812.

26 **Reboldi, A., Coisne, C., Baumjohann, D., Benvenuto, F., Bottinelli, D., Lira, S., Uccelli, A. et al.**, C-C chemokine receptor 6-regulated entry of TH-17 cells into the CNS through the choroid plexus is required for the initiation of EAE. *Nat. Immunol.* 2009. **10**: 514–523.

27 **Yamazaki, T., Yang, X. O., Chung, Y., Fukunaga, A., Nurieva, R., Pappu, B., Martin-Orozco, N. et al.**, CCR6 regulates the migration of inflammatory and regulatory T cells. *J. Immunol.* 2008. **181**: 8391–8401.

28 **Villares, R., Cadenas, V., Lozano, M., Almonacid, L., Zaballos, A., Martinez, A. C. and Varona, R.**, CCR6 regulates EAE pathogenesis by controlling regulatory CD4+ T-cell recruitment to target tissues. *Eur. J. Immunol.* 2009. **39**: 1671–1681.

29 **Loetscher, P., Pellegrino, A., Gong, J. H., Mattioli, I., Loetscher, M., Bardi, G., Baggiolini, M. et al.**, The ligands of CXC chemokine receptor 3, I-TAC, Mig, and IP10, are natural antagonists for CCR3. *J. Biol. Chem.* 2001. **276**: 2986–2991.

30 **Baron, J. L., Madri, J. A., Ruddle, N. H., Hashim, G. and Janeway, C. A., Jr.**, Surface expression of alpha 4 integrin by CD4 T cells is required for their entry into brain parenchyma. *J. Exp. Med.* 1993. **177**: 57–68.

31 **Keles, S., Charbonnier, L. M., Kabaleeswaran, V., Reisli, I., Genel, F., Gulez, N., Al-Herz, W. et al.**, Dedicator of cytokinesis 8 regulates signal transducer and activator of transcription 3 activation and promotes TH17 cell differentiation. *J. Allergy Clin. Immunol.* 2016. **138**: 1384–1394 e1382.

32 **Luci, C., Reynders, A., Ivanov, II, Cognet, C., Chiche, L., Chasson, L., Hardwigsen, J. et al.**, Influence of the transcription factor RORgammat on the development of NKp46+ cell populations in gut and skin. *Nat Immunol* 2009. **10**: 75–82.

33 **Singh, A. K., Eken, A., Fry, M., Bettelli, E. and Oukka, M.**, DOCK8 regulates protective immunity by controlling the function and survival of RORgammat+ ILCs. *Nat. Commun.* 2014. **5**: 4603.

34 **Rothhammer, V., Heink, S., Petermann, F., Srivastava, R., Claussen, M. C., Hemmer, B. and Korn, T.**, Th17 lymphocytes traffic to the central nervous system independently of alpha4 integrin expression during EAE. *J. Exp. Med.* 2011. **208**: 2465–2476.

35 **Brenner, D., Brustle, A., Lin, G. H., Lang, P. A., Duncan, G. S., Knobbe-Thomsen, C. B., St Paul, M. et al.**, Toso controls encephalitogenic immune responses by dendritic cells and regulatory T cells. *Proc. Natl. Acad. Sci. USA* 2014. **111**: 1060–1065.

36 **Oliaro, J., Van Ham, V., Sacirbegovic, F., Pasam, A., Bomzon, Z., Pham, K., Ludford-Menting, M. J. et al.**, Asymmetric cell division of T cells upon antigen presentation uses multiple conserved mechanisms. *J. Immunol.* 2010. **185**: 367–375.

37 **Brenner, D., Brechmann, M., Rohling, S., Tapernoux, M., Mock, T., Winter, D., Lehmann, W. D. et al.**, Phosphorylation of CARMA1 by HPK1 is critical for NF-kappaB activation in T cells. *Proc. Natl. Acad. Sci. USA* 2009. **106**: 14508–14513.

38 **Cossarizza, A., Chang, H.D., Radbruch, A., Andrä, I, Annunziato, F., Bacher, P., Barnaba, V. et al.**, Guidelines for the use of flow cytometry and cell sorting in immunological studies Eur. *J. Immunol.* 2017. **47**: 1584–1797.

Abbreviations: **DOCK8**: Dedicator Of Cytokinesis 8 · **GEF**: Guanine exchange factor · **LRCH1**: Leucine Rich Repeats And Calponin Homology Domain Containing 1 · **pri**: Primurus · **TCR**: T cell receptor · **Th**: T helper

Full correspondence: Dr. Anne Brüstle, The John Curtin School of Medical Research, The Australian National University, 131 Garran Rd, Acton ACT 2601, Australia
Fax: +61 2 6125 2595
E-mail: anne.bruestle@anu.edu.au